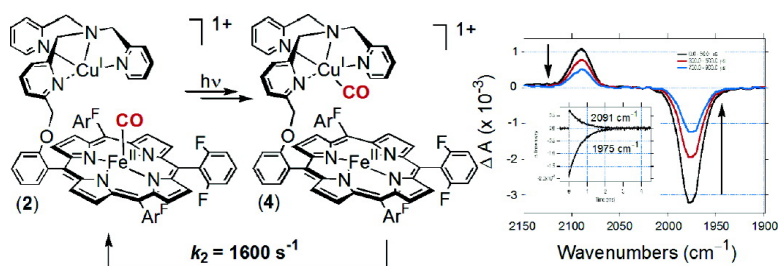


Photoinduced Carbon Monoxide Migration in a Synthetic Heme–Copper Complex

H. Christopher Fry, Andrew D. Cohen, John P. Toscano, Gerald J. Meyer, and Kenneth D. Karlin

J. Am. Chem. Soc., **2005**, 127 (17), 6225-6230 • DOI: 10.1021/ja043199e • Publication Date (Web): 12 April 2005

Downloaded from <http://pubs.acs.org> on March 25, 2009



More About This Article

Additional resources and features associated with this article are available within the HTML version:

- Supporting Information
- Links to the 1 articles that cite this article, as of the time of this article download
- Access to high resolution figures
- Links to articles and content related to this article
- Copyright permission to reproduce figures and/or text from this article

[View the Full Text HTML](#)

Photoinduced Carbon Monoxide Migration in a Synthetic Heme–Copper Complex

H. Christopher Fry, Andrew D. Cohen, John P. Toscano, Gerald J. Meyer, and Kenneth D. Karlin*

Contribution from the Department of Chemistry, The Johns Hopkins University, Baltimore, Maryland 21218

Received November 11, 2004; E-mail: karlin@jhu.edu

Abstract: Time-resolved infrared (TRIR) flash photolytic techniques have been employed to initiate and observe the efficient dissociation of CO from a synthetic heme-CO/copper complex, $[(^6\text{L})\text{Fe}^{\text{II}}(\text{CO})\cdot\text{Cu}]^+$ (**2**), in CH_3CN and acetone at room temperature. In CH_3CN , a significant fraction of the photodissociated CO molecules transiently bind to copper ($\nu_{\text{CO}}(\text{Cu}) = 2091 \text{ cm}^{-1}$) giving $[(^6\text{L})\text{Fe}^{\text{II}}\cdot\text{Cu}(\text{CO})]^+$ (**4**), with an observed rate constant, $k_1 = 1.5 \times 10^5 \text{ s}^{-1}$. That is followed by a slower direct transfer of CO from the copper moiety back to the heme ($\nu_{\text{CO}}(\text{Fe}) = 1975 \text{ cm}^{-1}$) with $k_2 = 1600 \text{ s}^{-1}$. Additional transient absorption (TA) UV-vis spectroscopic experiments have been performed monitoring the CO-transfer reaction by following the Soret band. Eyring analysis of the temperature-dependent data yields $\Delta H^\ddagger = 43.9 \text{ kJ mol}^{-1}$ for the **4**-to-**2** transformation, similar to that for CO dissociation from $[\text{Cu}(\text{tmpa})(\text{CO})]^+$ in CH_3CN ($\Delta H^\ddagger = 43.6 \text{ kJ mol}^{-1}$), suggesting CO dissociation from copper regulates the binding of small molecules to the heme within $[(^6\text{L})\text{Fe}^{\text{II}}\cdot\text{Cu}]^+$ (**3**). Our observations are analogous to those observed for the heme_{a3}/Cu_B active site of cytochrome *c* oxidase, where photodissociated CO from the heme_{a3} site immediately (ps) transfers to Cu_B followed by millisecond transfer back to the heme.

Introduction

Heme–copper oxidases (HCOs), which includes cytochrome *c* oxidase (CcO), catalyze the four-electron reduction of dioxygen to water, coupling this process to membrane proton translocation; the proton gradient is subsequently utilized by ATP synthase.^{1–4} The catalytic active site includes a hetero-bimetallic heme–copper (heme_{a3}/Cu_B) center (Figure 1).⁵ Photoinitiated dissociation of carbon monoxide (CO) from the reduced active site derivative of heme_{a3}, followed by O₂ reaction (Figure 2), has been employed as a major experimental tool or protocol to provide insight into the course of dioxygen reaction and nature of O₂-derived intermediates.^{6–12} More than that, CO

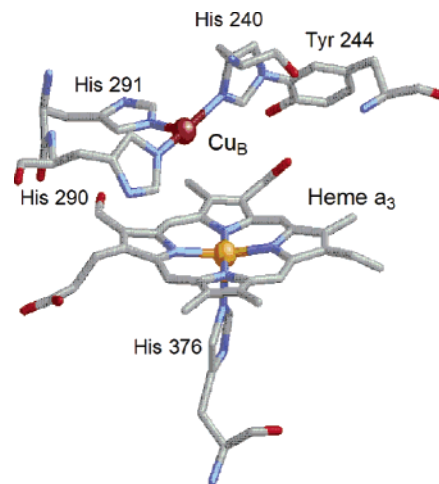


Figure 1. Structure of the fully reduced (heme_{a3}/Cu_B) active site of bovine cytochrome *c* oxidase, Fe...Cu = 5.19 Å.

photodissociation has found extensive application to probing HCO structure and mechanism by monitoring active site ligation changes,^{13–18} probing differences in active site structure between

- (1) Babcock, G. T. *Proc. Natl. Acad. Sci., U.S.A.* **1999**, *96*, 12971–12973.
- (2) In *Biochim. Biophys. Acta-Bioenergetics: Special Issue Dedicated to Jerry Babcock*; Tommos, C., Brzezinski, P., Ehrenberg, A., Eds., 2004; Vol. 1655, pp 1–413.
- (3) Ferguson-Miller, S.; Babcock, G. T. *Chem. Rev.* **1996**, *96*, 2889–2907.
- (4) Michel, H.; Behr, J.; Harrenga, A.; Kann, A. *Annu. Rev. Biophys. Biomol. Struct.* **1998**, *27*, 329–356.
- (5) Tsukihara, T.; Aoyama, H.; Yamashita, E.; Tomizaki, T.; Yamaguchi, H.; Shinzawa-Itoh, K.; Nakashima, R.; Yaono, R.; Yoshikawa, S. *Science* **1996**, *272*, 1136–1144.
- (6) Gibson, Q. H.; Greenwood, C. *Biochem. J.* **1963**, *86*, 541–554.
- (7) Greenwood, C.; Gibson, Q. H. *J. Biol. Chem.* **1967**, *242*, 1782–1787.
- (8) Szundi, I.; Liao, G.-L.; Einarsson, O. *Biochemistry* **2001**, *40*, 2332–2339.
- (9) Hill, B. C. *Biochemistry* **1996**, *35*, 6136–6143.
- (10) Oliveberg, M.; Malmström, B. G. *Biochemistry* **1992**, *31*, 3560–3563.
- (11) Babcock, G. T.; Floris, R.; Nilsson, T.; Pressler, M.; Varotsis, C.; Vollenbroek, E. *Inorg. Chim. Acta* **1996**, *243*, 345–353.
- (12) (a) Ogura, T.; Kitagawa, T. *Biochim. Biophys. Acta* **2004**, *1655*, 290–297. (b) Kitagawa, T.; Ogura, T. *Prog. Inorg. Chem.* **1997**, *45*, 431–479. (c) Ogura, T.; Takahashi, S.; Hirota, S.; Shinzawa-Itoh, K.; Yoshikawa, S.; Appelman, E. H.; Kitagawa, T. *J. Am. Chem. Soc.* **1993**, *115*, 8527–8536. (d) Ogura, T.; Takahashi, S.; Shinzawa-Itoh, K.; Yoshikawa, S.; Kitagawa, T. *J. Am. Chem. Soc.* **1990**, *112*, 5630–5631.

- (13) Alben, J. O.; Moh, P. P.; Fiamingo, F. G.; Altschuld, R. A. *Proc. Natl. Acad. Sci. U.S.A.* **1981**, *78*, 234–237.
- (14) (a) Einarsson, O.; Dyer, R. L.; Lemon, D. D.; Killough, P. M.; Hubig, S. M.; Atherton, S. J.; López-Garriga, J. J.; Palmer, G.; Woodruff, W. H. *Biochemistry* **1993**, *32*, 12013–12024. (b) Dyer, R. B.; Peterson, K. A.; Stoutland, P. O.; Woodruff, W. H. *Biochemistry* **1994**, *33*, 500–507.
- (15) Schelvis, J. P. M.; Deinum, G.; Varotsis, C. A.; Ferguson-Miller, S.; Babcock, G. T. *J. Am. Chem. Soc.* **1997**, *119*, 8409–8416.
- (16) Koutsoupakis, C.; Soulimane, T.; Varotsis, C. *J. Am. Chem. Soc.* **2003**, *125*, 14728–14732.

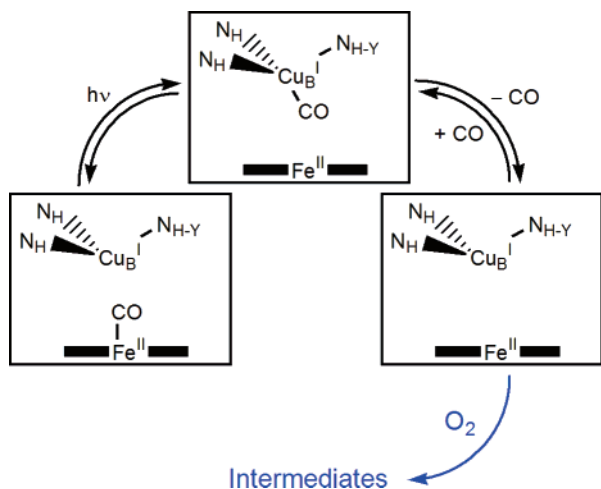
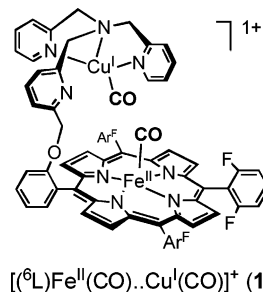


Figure 2. Mechanism of CO transfer in cytochrome *c* oxidase induced by photolysis of the carbonmonoxy–heme_{a3} species followed by the binding and processing of dioxygen.

HCOs from different species or sources,^{19–23} coupling heme–Cu ligation changes to protonation/deprotonation events of amino acid carboxyl groups related to proton translocation events,^{24–27} and even providing information about channels for O₂ active-site access.^{28–30} Gibson pioneered the use of CO photodissociation in heme proteins including cytochrome *c* oxidase,⁶ while Woodruff and co-workers^{14,31} first employed time-resolved infrared spectroscopic probing to reveal the fate of CcO photodissociated CO, in detail, following initial key observations by Alben and co-workers.¹³

Our own efforts,^{32–35} and those of others,^{32,36–39} have aimed at establishing basic insights into the chemistry of both O₂ and

CO with heme–copper centers. The focus of this report is on carbon monoxide binding and photochemistry in a heme–copper assembly, to provide fundamental background information concerning small molecule ligand binding in a heme–copper environment. We previously described the bis-CO complex [(⁶L)Fe^{II}(CO)₂..Cu^I(CO)]⁺ (**1**) (diagram), with $\nu_{\text{CO}}(\text{Fe}) = 1975 \text{ cm}^{-1}$ and $\nu_{\text{CO}}(\text{Cu}) = 2091 \text{ cm}^{-1}$.³⁴



To provide background chemistry needed for photochemical studies on this system, we have previously carried out and published investigations of CO photodissociation and recombination from individual synthetic heme⁴⁰ and copper⁴¹ components. The results indicate that bimolecular rate constants for CO binding to [Cu^I(tmpa)(Solvent)]⁺ {tmpa = tris(2-pyridylmethyl)amine, the same tetradentate ligand for copper(I) in (**1**)} ($k_{\text{CO}} = 10^7\text{--}10^9 \text{ M}^{-1}\text{s}^{-1}$)^{40,41} greatly exceed those for synthetic hemes ($k_{\text{CO}} = 10^5\text{--}10^7 \text{ M}^{-1}\text{s}^{-1}$).⁴² However, the binding of CO in [Cu^I(tmpa)(CO)]⁺ is not thermodynamically favored ($K_{\text{CO}}(\text{Cu}) = 10^2 \text{ M}^{-1}$)⁴³ when compared to that for iron(II)-porphyrinates such as (F₈)Fe^{II} {F₈ = tetrakis(2,6-difluorophenyl)-porphyrinate(2-)} and related compounds ($K_{\text{CO}}(\text{Fe}) > 10^9 \text{ M}^{-1}$),⁴² especially in the presence of competing coordinating solvents (i.e. CH₃CN). This finding is consistent with that observed for the HCO's (vide supra), where upon photorelease from the heme, CO rapidly switches from heme a₃ to Cu^I(ps), equilibrates (between bound and unbound Cu–CO forms), and subsequently returns to the heme on a millisecond time-scale (Figure 2).^{13,16,20,21,27,31} Here, in the first model system directed at such chemistry, we demonstrate that we can mimic this CO photodissociation, ligation first to copper and then rebinding to the heme.

Experimental Section

Synthesis. [(⁶L)Fe^{II}(thf)(CO)₂..Cu^I(CO)]B(C₆F₅)₄ (**1**)•[B(C₆F₅)₄]. While previously generated as a solution species,³⁴ we report here the synthesis and isolation of a solid form. In an inert, nitrogen atmosphere glovebox, (⁶L)Fe^{II} (101 mg, 9.2 × 10^{−5} mol) and [Cu^I(CH₃CN)₄]B-

- (17) Ohta, T.; Pinakoulaki, E.; Soulimane, T.; Kitagawa, T.; Varotsis, C. *J. Phys. Chem. B* **2004**, *108*, 5489–5491.
- (18) Liebl, U.; Lipowski, G.; Négre, M.; Lambry, J.-C.; Martin, J.-L.; Vos, M. H. *Nature* **1999**, *401*, 181–184.
- (19) Pitcher, R. S.; Watmough, N. J. *Bba-Bioenergetics* **2004**, *1655*, 388–399.
- (20) Pinakoulaki, E.; Soulimane, T.; Varotsis, C. *J. Biol. Chem.* **2002**, *277*, 32867–32874.
- (21) Giuffrè, A.; Forte, E.; Antonini, G.; D'Itri, E.; Brunori, M.; Soulimane, T.; Buse, G. *Biochem.* **1999**, *38*, 1057–1065.
- (22) Stavrakis, S.; Koutsoupakis, K.; Pinakoulaki, E.; Urbani, A.; Saraste, M.; Varotsis, C. *J. Am. Chem. Soc.* **2002**, *124*, 3814–3815.
- (23) Koutsoupakis, K.; Stafarakis, S.; Pinakoulaki, E.; Soulimane, T.; Varotsis, C. *J. Biol. Chem.* **2002**, 32860–32866.
- (24) Puustinen, A.; Bailey, J. A.; Dyer, R. B.; Mecklenburg, S. L.; Wikström, M.; Woodruff, W. H. *Biochemistry* **1997**, *36*, 13195–13200.
- (25) Okuno, D.; Iwase, T.; Shinzawa-Itoh, K.; Yoshikawa, S.; Kitagawa, T. *J. Am. Chem. Soc.* **2003**, *125*, 7209–7218.
- (26) McMahon, B. H.; Fabian, M.; Tomson, F.; Causgrove, T. P.; Bailey, J. A.; Rein, F. N.; Dyer, R. B.; Palmer, G.; Gennis, R. B.; Woodruff, W. H. *BBA-Bioenergetics* **2004**, *1655*, 321–331.
- (27) Rost, B.; Behr, J.; Hellwig, P.; Richter, O.-M. H.; Ludwig, B.; Michel, H.; Mantele, W. *Biochemistry* **1999**, *38*, 7565–7571.
- (28) Koutsoupakis, C.; Pinakoulaki, E.; Stavrakis, S.; Daskalakis, V.; Varotsis, C. *Biochim. Biophys. Acta - Bioenergetics* **2004**, *1655*, 347–352.
- (29) Lemon, D. D.; Calhoun, M. W.; Gennis, R. B.; Woodruff, W. H. *Biochemistry* **1993**, *32*, 11953–11956.
- (30) Salomonsson, L.; Lee, A.; Gennis, R. B.; Brzezinski, P. *Proc. Natl. Acad. Sci. U.S.A.* **2004**, *101*, 11617–11621.
- (31) Woodruff, W. H. *J. Bioenerg. Biomembr.* **1993**, *25*, 177–188.
- (32) Kim, E.; Chufan, E. E.; Kamaraj, K.; Karlin, K. D. *Chem. Rev.* **2004**, *104*, 1077–1133.
- (33) Kim, E.; Helton, M. E.; Wasser, I. M.; Karlin, K. D.; Lu, S.; Huang, H. W.; Moenne-Loccoz, P.; Incarvito, C. D.; Rheingold, A. L.; Honecker, M.; Kaderli, S.; Zuberbühler, A. D. *Proc. Natl. Acad. Sci., U.S.A.* **2003**, *100*, 3623–3628.
- (34) Kretzer, R. M.; Ghiladi, R. A.; Lebeau, E. L.; Liang, H.-C.; Karlin, K. D. *Inorg. Chem.* **2003**, *42*, 3016–3025.
- (35) Kim, E.; Shearer, J.; Lu, S.; Moenne-Loccoz, P.; Helton, M. E.; Kaderli, S.; Zuberbühler, A. D.; Karlin, K. D. *J. Am. Chem. Soc.* **2004**, *126*, 12716–12717.
- (36) Collman, J. P.; Sunderland, C. J.; Berg, K. E.; Vance, M. A.; Solomon, E. I. *J. Am. Chem. Soc.* **2003**, *125*, 6648–6649.
- (37) Chishiro, T.; Shimazaki, Y.; Tani, F.; Tachi, Y.; Naruta, Y.; Karasawa, S.; Hayami, S.; Maeda, Y. *Angew. Chem., Int. Ed.* **2003**, *42*, 2788–2791.

- (38) Collman, J. P.; Boulatov, R.; Sunderland, C. J.; Fu, L. *Chem. Rev.* **2004**, *104*, 561–588.
- (39) Boulatov, R. *Pure Appl. Chem.* **2004**, *76*, 303–319.
- (40) Thompson, D. W.; Kretzer, R. M.; Lebeau, E. L.; Scaltrito, D. V.; Ghiladi, R. A.; Lam, K.-C.; Rheingold, A. L.; Karlin, K. D.; Meyer, G. J. *Inorg. Chem.* **2003**, *42*, 5211–5218.
- (41) Scaltrito, D. V.; Fry, H. C.; Showalter, B. M.; Thompson, D. W.; Liang, H.-C.; Zhang, C. X.; Kretzer, R. M.; Kim, E.-i.; Toscano, J. P.; Karlin, K. D.; Meyer, G. J. *Inorg. Chem.* **2001**, *40*, 4514–4515.
- (42) Collman, J. P.; Brauman, J. I.; Iverson, B. L.; Sessler, J.; Morris, R. M.; Gibson, Q. H. *J. Am. Chem. Soc.* **1983**, *105*, 3052–3064.
- (43) We are separately studying in detail the kinetics of CO binding to various ligand-copper(I) complexes (via photoinitiated CO release and rebinding studied by transient absorption spectroscopy), and the results indicate very rapid reactions, faster or on par with hemes, as well as low equilibrium binding constants.
- (44) (a) Ghiladi, R. A.; Karlin, K. D. *Inorg. Chem.* **2002**, *41*, 2400–2407. (b) Ghiladi, R. A.; Kretzer, R. M.; Guzei, I.; Rheingold, A. L.; Neuhold, Y.-M.; Hatwell, K. R.; Zuberbühler, A. D.; Karlin, K. D. *Inorg. Chem.* **2001**, *40*, 5754–5767.

(C₆F₅)₄)⁴⁵ (84 mg, 9.2×10^{-5} mol) were placed in a 150 mL Schlenk flask equipped with a stir bar and capped with a 14/20 rubber septum. After removing the flask from the glovebox, carbon monoxide was purged through the flask, thus resulting in a presumed atmosphere of CO. Next, an air-free addition funnel containing 7 mL of THF was connected to the flask and CO was sparged through the solvent for 10 min before it was added to the solid mixture. Upon addition and mixing of the CO saturated THF to the solids in the flask, a bright red solution developed. Then, CO was sparged (60 min) through 120 mL heptane in the air-free addition funnel and was added to the heme–copper complex solution crashing out a purple solid. (Note: In order for CO to remain bound to the metal complex, the solid must be precipitated under a CO atmosphere. Removing THF solvent by vacuum results in partial to complete loss of coordinated CO.) Stirring was ceased and time was allowed for the solid to settle at the bottom of the flask. Finally, the supernatant was removed via cannula and the solid remaining was dried in vacuo for 30 min yielding 140 mg (80%) of desired product. IR: Nujol mull, ν_{CuCO} : 2096 cm⁻¹ and ν_{FeCO} : 1965 cm⁻¹. Anal. Calcd.: C, 56.83; H, 2.46; N, 5.70. Found: C, 57.10; H, 2.19; N, 5.21.

UV–Visible Spectroscopy. Absorption spectra were obtained using a Hewlett-Packard 8452A or a Hewlett-Packard 8453 diode array spectrophotometer. Low-temperature measurements (−80 to 0 °C) were made using a Neslab Ult-95 controller by circulating methanol through a two window optical dewar as previously described.

Infrared Spectroscopy IR spectra were obtained at room temperature using a Mattson Galaxy 4030 series FT-IR spectrophotometer. Samples were prepared in the drybox. 8–10 mg of compound made into a Nujol mull were pressed between two sodium chloride plates in the glovebox. Solution IR of carbonylated species were prepared in the glovebox by dissolving 8–10 mg in < 1 mL of solvent (CH₃CN or THF). The samples were brought out of the glovebox purged with CO for ~10 s at room temperature and reintroduced into the glovebox where the sample was transferred to a KBr plate solution-IR cell.

Flash Photolysis: Time-Resolved UV–Visible Spectroscopy (TA). Transient absorbance measurements were performed using an Nd:YAG (Continuum Surelite III) laser on a previously described apparatus.⁴⁶ Samples of [(⁶L)Fe^{II}(CO)₂Cu^I(CO)]B(C₆F₅)₄ (**1**)•[B(C₆F₅)₄] dissolved in acetone or acetonitrile prepared in the glovebox were irradiated with 355 or 532 nm pulsed light at 2–10 mJ/cm². The sample was protected from the probe beam with appropriate UV filters. For full transient absorption spectra, 0.5–3 μM samples were used in a 1.0 cm path length cuvette and kinetic traces were monitored from 320 to 650 nm with varying steps (every five to 10 nm) averaging 40 transients per wavelength. Initial and final absorbance values (A₀ and A_f, respectively) were extrapolated from the first-order kinetic fits from ORIGIN.

Using the same complex concentration as above, the CO concentration was varied in all solvents studied in order to determine bimolecular rate constants, k_{CO} (M⁻¹ s⁻¹). CO was varied (1 to 10 mM in 1 mM steps) as previously⁴⁷ described using a gas mixer. Four wavelengths were monitored in the Soret region averaging 60–120 transients per wavelength and the observed rate constants were averaged at each CO concentration studied. Plotting the observed rate constants, k_{obs} , versus CO concentration result in a straight line, eq 1 (Figure 4). The slope corresponds to the bimolecular rate of recombination, k_{CO} (M⁻¹ s⁻¹).

$$k_{\text{obs}} = k_{\text{CO}}[\text{CO}] \quad (1)$$

To study the effect of complex concentration on the observed first-order rate constants, samples ranging from 1 to 700 μM [(⁶L)Fe^{II}(CO)₂Cu^I(CO)]B(C₆F₅)₄ (**1**)•[B(C₆F₅)₄] in acetone, acetonitrile or

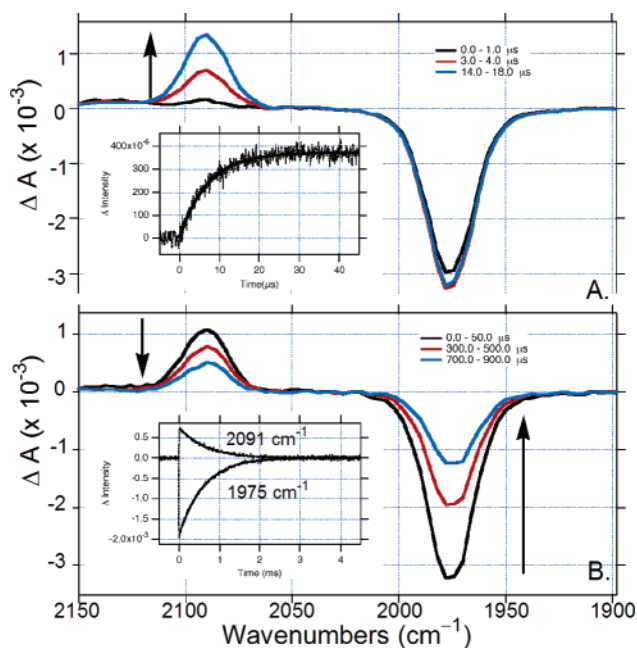


Figure 3. TRIR difference spectra representing the photolysis ($\lambda_{\text{ex}} = 355$ nm) of [(⁶L)Fe(CO)₂Cu]⁺ (**2**) in CH₃CN (1.6 mM): (A) Time period: 0–18 μs. CO is dissociated from the heme ($\nu_{\text{CO}}(\text{Fe}) = 1975$ cm⁻¹) and subsequently binds to copper ($\nu_{\text{CO}}(\text{Cu}) = 2091$ cm⁻¹). Various time delays are displayed by black, 0–1.0 μs; red, 3.0–4.0 μs; and blue lines, 14.0–18.0 μs. The inset is a kinetic trace taken at 2091 cm⁻¹ displayed with a first-order fit ($k_1 = 1.5 \times 10^5$ s⁻¹). (B) Time period: 20–900 μs. CO transfers from copper ($\nu_{\text{CO}}(\text{Cu}) = 2091$ cm⁻¹) back to heme ($\nu_{\text{CO}}(\text{Fe}) = 1975$ cm⁻¹). Various time delays are displayed by black, 20–50 μs; red, 300–500 μs; and blue lines, 700–900 μs. The inset contains two kinetic traces taken at 1975 and 2091 cm⁻¹ displayed with a first-order fit ($k_2 = 1500$ s⁻¹).

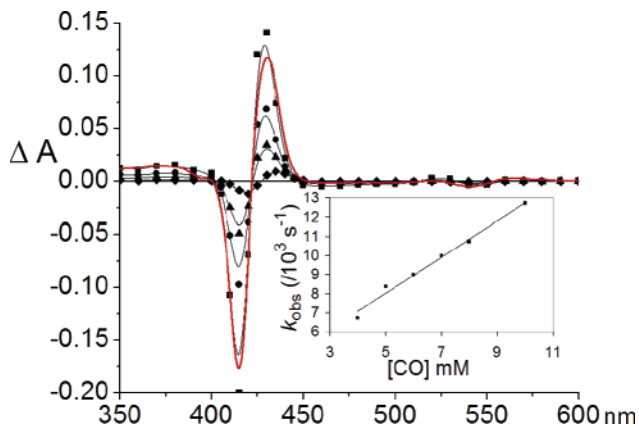


Figure 4. Time-resolved absorption spectra recorded after pulsed 532 nm light excitation of [(⁶L)Fe^{II}(CO)₂Cu^I(CO)]⁺ in CH₃CN at room temperature under 1 atm CO. The data are shown at delay times of 10 ns (squares), 5 μs (circles), 10 μs (triangles), and 30 μs (diamonds). A spectrum simulated as (Abs[(⁶L)Fe^{II}·Cu]⁺ (**3**) – Abs[(⁶L)Fe^{II}(CO)₂Cu^I(CO)]⁺ (**1**)) is overlaid in red. The inset represents the CO concentration dependence on k_{obs} for the post-photolytic CO recombination with [(⁶L)Fe^{II}·Cu^I(CO)]⁺.

tetrahydrofuran were prepared in quartz Schlenk cuvettes with 2 or 10 mm path length in the glovebox and irradiated as described above. Four wavelengths were monitored averaging 60 transient kinetic traces in the Soret region or α-region depending on the concentration studied averaging 60 transient kinetic traces per wavelength. Kinetic analysis was performed using ORIGIN (vide supra) and the four observed rate constants were fit as first-order processes and averaged at each concentration studied.

Temperature-dependent studies on the observed rate constants, k_{obs} , were performed at high concentrations (500 μM) of [(⁶L)Fe^{II}(CO)₂Cu^I(CO)]⁺.

(45) Liang, H.-C.; Kim, E.; Incarvito, C. D.; Rheingold, A. L.; Karlin, K. D. *Inorg. Chem.* **2002**, *41*, 2209–2212.

(46) Argazzi, R.; Bignozzi, C. A.; Heimer, T. A.; Castellano, F. N.; Meyer, G. J. *J. Phys. Chem.* **1994**, *33*, 5741–5749.

(47) Fry, H. C.; Scaltrito, D. V.; Karlin, K. D.; Meyer, G. J. *J. Am. Chem. Soc.* **2003**, *125*, 11866–11871.

(CO)]B(C₆F₅)₄ (1)•[B(C₆F₅)₄] in acetone and CH₃CN. Samples were prepared in the glovebox and 2 mm cuvettes had to be used at such large concentrations. Temperature was varied from 233 to 273 K using a Neslab Ult-95 controller by circulating methanol through a four-window optical dewar as previously described.⁴⁷ Room temperature (298 K) measurements were included in the analysis. Eyring analysis was utilized to afford the enthalpic and entropic barriers, eq 2.

$$\ln(k_{\text{obs}} \times h)/(k_{\text{B}} \times T) = -\Delta H^{\ddagger}/RT + \Delta S/R \quad (2)$$

Flash Photolysis: Time-Resolved Infrared (TRIR) Spectroscopy.

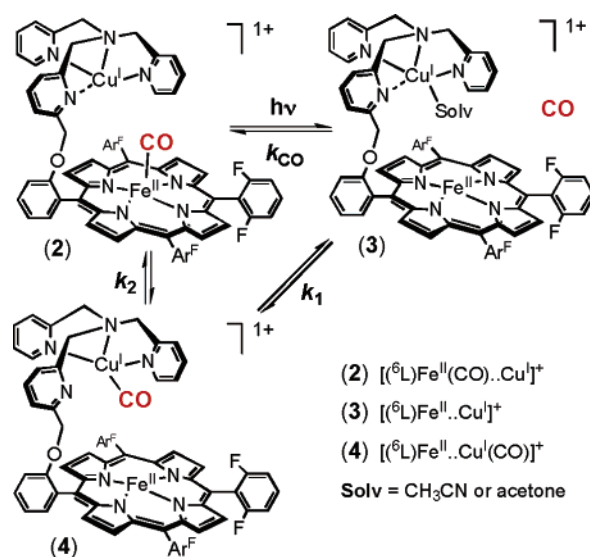
TRIR measurements were performed using a Q-switched Quantronix Nd:YAG (355 nm, 90 ns pulsewidth, 0.4 mJ/pulse, operating at 200 Hz) laser on a previously described apparatus.⁴⁸ Samples of [(⁶L)Fe^{II}-(CO)..Cu^I(CO)]B(C₆F₅)₄ (1)•[B(C₆F₅)₄] in acetone (1.6 mM) and acetonitrile (0.5–1.6 mM) were prepared in the glovebox in 10 mL Schlenk tubes or flasks equipped with a 14/20 rubber septum. Ten mL were needed as a flow-cell is used in this apparatus. The flow cell was composed of CaF₂ plates with a path-length (*l*) of 0.5 mm. (Note: TA spectroscopy did not require a flow cell as the samples were irradiated at 1 Hz. TRIR irradiation occurs at 200 Hz.) During the experiments the samples were placed under a positive pressure of Argon in order to slow decomposition due to dioxygen exposure. With many of the efforts taken to alleviate exposure to dioxygen, a complete air-free flow-cell was never devised. Nevertheless, the samples were irradiated with 355 nm pulsed light. A full TRIR spectrum was taken from 1900 to 2150 cm⁻¹ monitoring every 4 cm⁻¹. Kinetic traces were monitored at the respective ν_{CO} (cm⁻¹) for the carbonyl when bound to copper (2091 cm⁻¹) and iron (1968 cm⁻¹ in acetone while 1975 cm⁻¹ in CH₃CN {Note, these are six-coordinate solvent ligated (solvent)Fe^{II}(CO) complexes; the difference in ν_{CO} derives from the differences in axial ligand base}^{34,44}) averaging 400–800 transients. All traces were fit to a first-order kinetic model.

Results

When [(⁶L)Fe(CO)..Cu(CO)]⁺ (1) is dissolved in CH₃CN, the solvent displaces the copper bound carbon monoxide, as indicated by the complete loss of the $\nu_{\text{CO}}(\text{Cu}) = 2091 \text{ cm}^{-1}$ band of the solution phase FTIR spectrum.⁴⁹ ¹H NMR and FTIR spectroscopy indicate that CO remains coordinated to the heme, giving [(⁶L)Fe(CO)..Cu]⁺ (2), $\delta_{\text{pyrrole}}(\text{CD}_3\text{CN}) = 8.9 \text{ ppm}$ and $\nu_{\text{CO}}(\text{Fe}) = 1975 \text{ cm}^{-1}$, Scheme 1. Thus, as is well established in copper(I) coordination chemistry,^{50,51} acetonitrile acts as a strong ligand and displaces the CO.

Upon single wavelength excitation ($\lambda_{\text{ex}} = 355 \text{ nm}$) of [(⁶L)Fe^{II}(CO)..Cu]⁺ (2) at room temperature in CH₃CN (1.6 mM) as monitored by TRIR, an immediate loss of the $\nu_{\text{CO}}(\text{Fe}) = 1975 \text{ cm}^{-1}$ peak occurs, consistent with the loss of CO from the iron center, thus forming [(⁶L)Fe^{II}..Cu]⁺ (3) and free CO (Scheme 1 & Figure 3A). Comparative actinometry indicates a $\phi = 1.0 \pm 0.2$ for this process, consistent with other measurements of CO release from hemes.^{52–54} The CO does not transfer directly to the copper center as in HCOs, but once liberated

Scheme 1



(into solvent) via photoejection, it binds to the copper(I) center with an observed rate constant, k_1 (CH₃CN) = $1.2 \times 10^5 \text{ s}^{-1}$ (Figure 3A and Scheme 1), corresponding to the formation of [(⁶L)Fe^{II}..Cu^I(CO)]⁺ (4) where $\nu_{\text{CO}}(\text{Cu}) = 2091 \text{ cm}^{-1}$, consistent with the tmpa moiety supporting copper in a tridentate (N₃) mode (Scheme 1).³⁴ The first-order nature of this process is attributed to the presence of a composite mechanism, including solvent dissociation and CO binding. Dioxygen binding to [Cu^I-(tmpa)(RCN)]⁺ also appears to proceed through a dissociative mechanism.^{55,56} To provide complementary information in another (less strongly) potentially coordinating solvent, we repeated this study in acetone. Similar chemistry occurs, photodissociation of CO and binding to Cu, with an only slightly enhanced rate constant, k_1 (acetone) = $6.5 \times 10^5 \text{ s}^{-1}$.⁴⁹

Relative absorptivities (based on IR spectra of fully formed [(⁶L)Fe^{II}(CO)..Cu^I(CO)]⁺ (1)) indicate that approximately 60% of the photodissociated CO binds to the copper forming [(⁶L)Fe^{II}..Cu^I(CO)]⁺ (4) whereas the other portion remains free in solution. At this point, the Cu-bound CO molecule transfers directly to the iron as indicated by the simultaneous loss of $\nu_{\text{CO}}(\text{Cu}) = 2091 \text{ cm}^{-1}$ and the reconstitution of $\nu_{\text{CO}}(\text{Fe}) = 1975 \text{ cm}^{-1}$ (k_2 (CH₃CN) = $1500 \pm 150 \text{ s}^{-1}$) (Figure 3B). Thus, the starting complex [(⁶L)Fe^{II}(CO)..Cu]⁺ (2) is reformed in an overall reversible process (Scheme 1). Changing to acetone as solvent gives a roughly similar result, k_2 (acetone) = $2000 \pm 200 \text{ s}^{-1}$.⁴⁹

In additional experiments carried out using TRIR spectroscopy, we noticed that with lower concentrations of [(⁶L)Fe^{II}-(CO)..Cu]⁺ (2), much less than 60% (see above) of CO transfer to Cu occurred. Follow-up experiments using transient absorption UV–vis spectroscopy ($\lambda_{\text{ex}} = 532 \text{ nm}$, 298 K) monitoring in the intense Soret band (λ_{mon} varied from 425 to 435 nm) were carried out. In the range 1–200 μM , there is a roughly linear dependence of the observed rate constant upon [(2)],⁴⁹ for recombination of CO with heme (in a second-order process), thus with no assistance via prior binding to the copper ion center (as indicated by the lack of $\nu_{\text{CO}}(\text{Cu})$ in the TRIR

(48) Wang, Y. H.; Yuzawa, T.; Hamaguchi, H. O.; Toscano, J. P. *J. Am. Chem. Soc.* **1999**, *121*, 2875–2882.

(49) See Supporting Online Material.

(50) Jardine, F. H. *Adv. Inorg. Chem. Radiochem.* **1975**, *17*, 115–163.

(51) Hathaway, B. J. In *Comprehensive Coordination Chemistry*; Wilkinson, G., Ed.; Pergamon: New York, 1987; Vol. 5, pp 533–774.

(52) Antonini, E.; Brunori, M. *Hemoglobin and Myoglobin in Their Reactions with Ligands*; North-Holland Publishing Co.: Amsterdam, 1971.

(53) Brunori, M.; Giacomini, G.; Antonini, E.; Wyman, J. *Proc. Natl. Acad. Sci. U.S.A.* **1973**, *70*, 3141–3144.

(54) Gibson, Q. H.; Olson, J. S.; McKinnin, R. E.; Rohlfis, R. J. *J. Biol. Chem.* **1986**, *261*, 228–239.

(55) Karlin, K. D.; Kaderli, S.; Zuberbühler, A. D. *Acc. Chem. Res.* **1997**, *30*, 139–147.

(56) Zhang, C. X.; Kaderli, S.; Costas, M.; Kim, E.-i.; Neuhold, Y.-M.; Karlin, K. D.; Zuberbühler, A. D. *Inorg. Chem.* **2003**, *42*, 1807–1824.

Table 1. Kinetic Parameters for CO Binding Processes Following Photodissociation from $[(^6\text{L})\text{Fe}^{\text{II}}(\text{CO})\text{Cu}]^+$ (**2**) (Scheme 1): k_1 , CO Binding to the Copper Ion in $[(^6\text{L})\text{Fe}^{\text{II}}\text{Cu}]^+$ (**3**); k_2 , Subsequent CO Transfer from Copper to Iron^a

parameter	CH ₃ CN	acetone	CcO
k_1 (RT, s ⁻¹)	1.5×10^5	6.5×10^5	$> 10^{9c}$
k_2 (298 K, s ⁻¹) ^b	900 ± 100	1200 ± 100	1030^c
ΔH^\ddagger (kJ mol ⁻¹)	43.9	45.1	41.8 ^c
ΔS^\ddagger (J mol ⁻¹ K ⁻¹)	-41	-35	-50 ^c
k_{CO} (RT, M ⁻¹ s ⁻¹)	$1.0 \pm 0.1 \times 10^7$	$3.1 \pm 0.2 \times 10^7$	4.4×10^{5d}

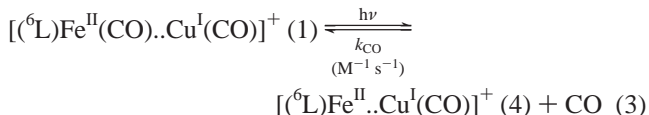
^a Carbon monoxide heme rebinding following photodissociation from $[(^6\text{L})\text{Fe}^{\text{II}}(\text{CO})\text{Cu}(\text{CO})]^+$ (**1**) is given by k_{CO} . Pertinent related enzyme (CcO) data is also provided. ^b Calculated from the activation parameters. ^c See ref 12. ^d See ref 28.

experiments). However, between 200 and 1600 μM in **[(2)]**, when the transient binding of CO to copper is observed to be significant and dominant, an intramolecular transfer of CO from Cu to heme independent of **[(2)]** is well described as k_2 (CH₃CN) = 1200 ± 100 s⁻¹ at room temperature, Scheme 1.^{49,57}

The temperature dependence of k_2 was probed in order to provide more insight into the mechanism of CO transfer from copper to iron. Eyring analysis for reaction in CH₃CN afforded activation parameters, $\Delta H^\ddagger = 43.9$ kJ mol⁻¹ and $\Delta S^\ddagger = -41$ J mol⁻¹ K⁻¹ (Table 1).⁴⁹ The rather large activation enthalpy is in fact nearly identical to that observed for the dissociation of CO from the closely related complex $[\text{Cu}^{\text{I}}(\text{tmpa})(\text{CO})]^+$, $\Delta H^\ddagger = 43.6$ kJ in CH₃CN;⁴⁹ this, of course, is the same moiety present in the ⁶L containing complexes (Scheme 1). As indicated by the entries in Table 1, there is little solvent dependence on the activation parameters (acetone versus CH₃CN) for the CO migration reaction.

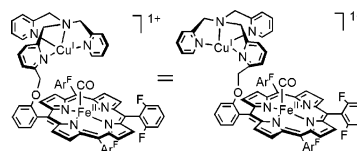
Photodissociation and binding experiments where excess CO was present in solution were also carried out. Here, the expectation was that both iron and copper centers in $[(^6\text{L})\text{Fe}^{\text{II}}\text{Cu}]^+$ (**3**) would be CO saturated, giving $[(^6\text{L})\text{Fe}^{\text{II}}(\text{CO})\text{Cu}(\text{CO})]^+$ (**1**), and that CO rebinding to the heme would thus *not* proceed via Cu(I) binding (as observed, *vide supra*; Scheme 1), since this site would be unavailable (with CO already present). Note that the 532 nm excitation used would not result in CO photoejection from the Cu^I(tmpa) moiety, as this requires 355 nm (i.e., higher energy) illumination.⁴¹ In fact, the findings here are in accord with expectation (eq 3): (1) With excess CO present, the transient difference spectrum generated after 532 nm excitation of $[(^6\text{L})\text{Fe}^{\text{II}}(\text{CO})\text{Cu}(\text{CO})]^+$ (**1**) resembles, with excellent agreement, the *calculated* difference spectrum of $\{[(^6\text{L})\text{Fe}^{\text{II}}\text{Cu}]^+ - [(\text{L})\text{Fe}^{\text{II}}(\text{CO})\text{Cu}(\text{CO})]^+\}$,⁵⁸ Figure 4, indicating CO is photoejected from the heme, and (2) when the CO concentration is varied, a linear dependence on [CO] is observed, and the slope of k_{obs} vs [CO] plot yields the bimolecular rate constant for CO recombination to the heme, $k_{\text{CO}} = 1.0 \pm 0.3 \times 10^7$ M⁻¹ s⁻¹ (eq 3; inset, Figure 4). This binding is in line with other literature values for CO recombination to ferrous hemes, and the process is clearly much faster than the CO rebinding which is mediated by Cu^I-tmpa ligation (*vide supra*). Under these conditions of excess CO and thus

where Cu is CO-bound, the copper plays no particular role in the overall process of CO binding to the heme. These conclusions are further supported by complementary TRIR experiments we have carried out, where we do not detect a Cu^I(tmpa)-CO moiety forming in the same time regime. As indicated, the Cu is already occupied by a molecule of CO. We have also carried out these experiments with excess CO in acetone as solvent, where very similar results are obtained, Table 1.⁴⁹



Discussion

The results of CO photodissociation chemistry demonstrated here with the heme–copper assembly $[(^6\text{L})\text{Fe}^{\text{II}}\text{Cu}]^+$ (**3**) provide both similarities and differences to what is observed in heme–copper oxidases. For example, cytochrome *caa3* oxidase transfers 100% of the photoreleased CO to the Cu_B site within 1 ps.¹⁴ However, subsequent equilibration results in 35% of the CO freely dissociated from the Cu_B site without binding to iron, leaving 65% of the CO bound to copper. Ultimately, all the CO returns to the heme, due to the thermodynamic preferences. In our model study, picosecond transfer to the copper metal is not observed (*vide supra*). We believe this is in part a result of the solvents employed in our model systems, which influence the binding of CO to copper(I) as a competitive ‘substrate’ capable of occupying the coordination site ultimately inhibiting the binding of CO to copper. Our attempt to address this issue was investigated by using solvents with varying degrees of coordinating ability (i.e., CH₃CN coordinates more readily to copper(I) than acetone). We observe a 4-fold enhancement of the observed rate constant corresponding to the formation of the Cu–CO bond (Table 1). Furthermore, one can presume that the flexible tethered portion of the ⁶L ligand, i.e., the Cu-tmpa moiety linked via a benzylic ether oxygen group, allows the copper to swing away from the heme site (see diagram). This would result in inefficient capture of the photoreleased CO and may further explain the inability of CO to transiently bind to copper at low concentrations. In the enzyme, of course, the juxtaposition of the copper to the heme_{a3} is fixed in the active site pocket.



Next, the transfer of CO directly from copper to iron in various heme–copper oxidases has measured rate constants, $k_2 = 10^1$ to 10^3 s⁻¹,^{13,16,20,21} reflecting differences in heme_{a3}/Cu_B active-site structure. Our values for CH₃CN and acetone solvents are (both) $k_2 = 10^3$ s⁻¹, thus comparing very well to the enzymes (Table 1). Overall, our results agree with the general principle that CO kinetically favors binding to copper(I) centers,^{41,43,47} at least as a detectable but transient species, prior to transfer to the heme, the thermodynamically favored iron–carbonyl product.

(57) Differences in observed rate constants (k_2) measured by TA and TRIR could be attributed to increased sample concentrations and lack of full temperature control.

(58) As we cannot isolate the complex $[(^6\text{L})\text{Fe}^{\text{II}}\text{Cu}(\text{CO})]^+$ the calculated difference spectrum utilized the isolable complex $[(^6\text{L})\text{Fe}^{\text{II}}\text{Cu}]^+$ because the spectra of these two complexes (from 350 to 600 nm) are within experimental error of one another (being dominated by the π - π^* transitions of the heme).

Furthermore, despite the simplicity of our model system, we can offer additional support for the notion discussed by others^{28–30} that Cu_B possesses a regulatory function in the delivery of O₂ (and CO) to the heme_{a3} portion of the HCO active sites. As described, the rate of CO binding to the heme after photoejection of carbon monoxide from the heme, but with excess CO present, is the same as the heme-only result;⁴⁰ this is because the copper is “tied up” by the excess CO. Essentially, a similar experiment has been carried out in an HCO; Cu_B removal from the active site of cytochrome *b₀* by protein modification (via site-directed mutagenesis)²⁹ also resulted in a greater rate of CO rebinding to heme_{a3}. Thus, the presence of a cuprous ion proximate to the heme, in enzymes and in our model system, slow the approach and binding of CO, and thus we presume O₂, to the heme. As discussed elsewhere in more detail, this may relate to the regulation and timing of proton translocation,^{24–27} electron transfer and/or O–O cleavage events.^{28–30}

We further note that we obtained activation parameters for the transfer of CO from the Cu-tmpa moiety to the heme, which remarkably coincide with those observed in one case for CcO (Table 1).¹³ The regulation or slowing in transferring of CO to the heme, at least in our model system, is thus largely controlled by the Cu^I–CO off rate. The significant activation enthalpy is associated with Cu^I–CO bond cleavage as suggested by the separate study and analysis of CO dissociation from the compound [Cu^I(tmpa)(CO)]⁺.⁴⁹ To reiterate, CO and O₂ binding to cuprous ions, at least Cu^I(tmpa), occurs extremely rapidly. Thus, the relatively slow rate of CO and O₂ binding to the heme in HCOs and our heme–copper assembly is due to an initial interaction and binding to copper. Concerning the observed negative reaction entropy of activation associated with CO transfer to iron (i.e., the *k*₂ step, Table 1, Scheme 1), we account for this by suggesting that in the transition state, the flexible tethered portion (see diagram, above) with Cu^I–CO moiety must now achieve a specific juxtaposition directly adjacent to the heme in order to transfer the carbon monoxide ligand.

Why do CO (and O₂) kinetically prefer copper(I) to iron(II), at least in the tmpa type ligand for copper, as studied here and previously?⁴⁷ It could be because five-coordinate high-spin reduced hemes undergo both a spin-state and structural change (i.e., movement of the iron ‘through’ the heme) upon binding of these diatomics. And in low-spin six-coordinate ferrous hemes, a ligand dissociation and a spin-state change must occur. No spin state considerations come into play for copper(I), and

the binding site is likely highly accessible. a simple addition reaction. Further experimental and theoretical work should be performed.

Conclusion

All in all, we have displayed mechanistic properties of CO binding to our model heme–copper, [(⁶L)Fe^{II}.Cu^I]⁺ complex that are strikingly similar to those of heme–copper oxidases: (1) carbon monoxide can be efficiently photodissociated ($\phi = 1.00$) from the heme, either in [(⁶L)Fe^{II}(CO)..Cu^I(CO)]⁺ (**1**) or [(⁶L)Fe^{II}(CO)..Cu^I]⁺ (**2**), (2) in [(⁶L)Fe^{II}(CO)..Cu^I]⁺ (**2**), in the absence of any additional CO in solution, carbon monoxide post-photolytically transfers mainly to copper, due to its inherently faster rate of binding to copper(I) than to reduced heme, (3) CO subsequently transfers on a millisecond time-scale to the heme in a fully reversible process, supporting the notion that heme-CO species are thermodynamically more stable than Cu^I–CO species, (4) when the copper site is preoccupied by CO under excess CO concentrations (effectively denying access of photoreleased CO to the copper ion), CO rebinding to the heme is faster than if the copper site was free, suggesting that under stoichiometric (1:1, CO:complex) conditions copper regulates the binding of CO to the heme, and (5) this regulation is due to the large enthalpic activation barrier of CO dissociating from copper(I). Additional studies comparing heme only, untethered heme–copper systems, and heme–copper species with varied copper ligand environments are underway.

Acknowledgment. We acknowledge support from the National Institute of Health (K.D.K.) and a National Science Foundation environmental research grant (CRAEMS, K.D.K., and G.J.M.). J.P.T. acknowledges support from the National Science Foundation (CHE-0209350), while A.D.C. is grateful for support from an ACS Organic Division Graduate Fellowship.

Supporting Information Available: Experimental for CO-binding to [Cu^I(tmpa)(CH₃CN)]⁺, figures for infrared spectra of the solid compound [(⁶L)Fe^{II}(CO)..Cu^I(CO)]B(C₆F₅)₄ (**1**)•[B(C₆F₅)₄] and in acetonitrile solvent, TRIR kinetic traces of [(⁶L)Fe^{II}(CO)..Cu^I]⁺ (**2**) in acetone, variable complex concentration versus *k*₂ in acetonitrile, Eyring plots corresponding to *k*₂, Van’t Hoff and Eyring plots for the binding and dissociation of CO to [Cu^I(tmpa)(CH₃CN)]⁺, and TA difference spectrum of [(⁶L)Fe^{II}(CO)..Cu^I(CO)]⁺ (**1**) in acetone under 1 atm CO. This material is available free of charge via the Internet at <http://pubs.acs.org>.

JA043199E